nature
structural &
molecular biology

Proton-powered subunit rotation in single membrane-bound F_0F_1-ATP synthase

Manuel Diez[1], Boris Zimmermann[1], Michael Börsch[2], Marcelle König[3], Enno Schweinberger[3], Stefan Steigmiller[1], Rolf Reuter[1], Suren Felekyan[3], Volodymyr Kudryavtsev[3], Claus A M Seidel[3] & Peter Gräber[1]

Synthesis of ATP from ADP and phosphate, catalyzed by F_0F_1-ATP synthases, is the most abundant physiological reaction in almost any cell. F_0F_1-ATP synthases are membrane-bound enzymes that use the energy derived from an electrochemical proton gradient for ATP formation. We incorporated double-labeled F_0F_1-ATP synthases from *Escherichia coli* into liposomes and measured single-molecule fluorescence resonance energy transfer (FRET) during ATP synthesis and hydrolysis. The γ subunit rotates stepwise during proton transport–powered ATP synthesis, showing three distinct distances to the b subunits in repeating sequences. The average durations of these steps correspond to catalytic turnover times upon ATP synthesis as well as ATP hydrolysis. The direction of rotation during ATP synthesis is opposite to that of ATP hydrolysis.

To clarify the central role of energy transduction and the rotary mechanism of F_0F_1-ATP synthase, much experimental work has focused on the mechanistic events in this molecular motor[1–17]. F_0F_1-ATP synthase catalyzes the formation of ATP from ADP and phosphate in bacteria, mitochondria and chloroplasts, and this reaction is driven by conversion of Gibbs free energy derived from a transmembrane electrochemical proton gradient[1]. The enzyme consists of two parts, F_1 and F_0, which in *E. coli* have the subunit composition $\alpha_3\beta_3\gamma\delta\varepsilon$ and ab_2c_n with an expected number n of c subunits between 10 and 12, respectively (**Fig. 1a**). ATP synthesis takes place at the three β subunits of F_1, which sequentially adopt different conformations during catalysis[2]. Due to different interactions of each β subunit with the γ subunit, three possible conformations of the catalytic binding sites are found in the X-ray structure[3]. A sequential conversion of the conformations of the catalytic sites is caused by rotation of the γ subunit, which is located in the center of the $\alpha_3\beta_3$ complex. Rotation of the γ subunit is assumed to be coupled mechanically to proton translocation by a rotational movement of the c-ring[4] of F_0. Therefore, the subunits are also defined as 'rotor' ($\gamma\varepsilon c_n$, **Fig. 1**) and 'stator' ($\alpha_3\beta_3\delta ab_2$, **Fig. 1**)[5–8].

In single immobilized F_1 subcomplexes, subunit rotation during ATP hydrolysis has been demonstrated by video-microscopic experiment using a fluorescent actin filament connected to the γ subunit as a marker of its orientation[9]. Hydrolysis of ATP led to rotation of the γ subunit in 120° steps. Recently, resolution of substeps[10,11] has shown that the binding event of ATP at a relative γ-subunit position of 0° (or 120° and 240°, respectively) and the catalytic processes of ATP hydrolysis and product release at a relative γ-subunit position between 80° and 90° are associated with different angular orientations of the γ subunit. The direction of rotation was counterclockwise when viewed from F_0 to F_1 (**Fig. 1b**). Actin-filament attachment has also been used to show rotation of the c subunits of F_0 using immobilized complexes[12,13]; and by a single-fluorophore polarization experiment[14]. 'Molecular dynamics' simulations of the direction of ATP synthesis showed induced conformational changes within F_1 when an external rotary force was applied to the γ subunit[15,16].

However, up to now the rotation of the central γ subunit during proton-powered ATP synthesis could only be demonstrated indirectly[17]. The following questions must be investigated: (i) can we observe a rotation of the γ subunit coupled to proton translocation during ATP synthesis, that is distinguishable from an oscillation mode between only two positions for the γ subunit? (ii) Is the direction of rotation during ATP synthesis opposite or identical to that during ATP hydrolysis; that is, is this enzyme a bidirectional or unidirectional motor? (iii) Is the movement of the γ subunit during proton translocation continuous or stepwise? Because consecutive conformational motions in protein machines are stochastic and thus can hardly be synchronized, the subunit movements in F_0F_1-ATP synthase must be studied at the single-molecule level. Here we present the use of intramolecular single-molecule FRET to observe the rotary movement of the γ subunit during proton-powered ATP synthesis by single F_0F_1-ATP synthase. The FRET donor was attached at the rotating γ subunit and the FRET acceptor crosslinked the nonrotating b-subunit dimer. During catalysis, fluctuating FRET efficiencies indicate the relative movement of the labels because their distances sequentially interchange as a result of the rotation of the γ subunit.

[1]Institut für Physikalische Chemie, Albert-Ludwigs-Universität Freiburg, Albertstrasse 23 a, 79104 Freiburg, Germany. [2]3. Physikalisches Institut, Universität Stuttgart, Pfaffenwaldring 57, 70569 Stuttgart, Germany. [3]Max-Planck-Institut für Biophysikalische Chemie, Am Fassberg 11, 37077 Göttingen, Germany. Correspondence should be addressed to M.B. (michael.boersch@physchem.uni-freiburg.de).

Published online 18 January 2004; doi:10.1038/nsmb718

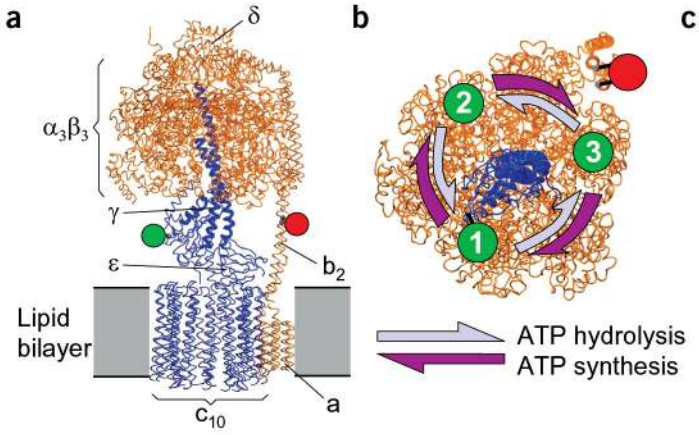

Figure 1 Model of F_0F_1 from *E. coli* (see Methods). (**a**) Side view. The FRET donor is bound to the γ subunit (green circle), the FRET acceptor Cy5bis to the b subunits (red circle). 'Rotor' subunits are blue, 'stator' subunits are orange. (**b**) Cross-section at the fluorophore level, viewed from F_0. Cy5bis (red) crosslinks the b subunits. Donor position 1 (green) of cysteine γ-T106C is farthest away from b-Q64C. Rotation of the γ subunit by 120° and 240° results in donor positions 2 and 3, respectively. (**c**) Photon bursts are observed when a freely diffusing single liposome with a single FRET-labeled F_0F_1 traverses the confocal detection volume (yellowish) within the laser focus (green).

RESULTS

Reconstituted F_0F_1-ATP synthase with FRET labels

To study intersubunit rotation of the membrane-bound F_0F_1-ATP synthase (referred to as F_0F_1 below) from *E. coli* under conditions of ATP synthesis and hydrolysis, the following prerequisites must be met: (i) preparation of the fully functional holoenzyme F_0F_1 in a quasi-native environment without additional immobilization; (ii) generation of a proton gradient across the lipid membrane; (iii) attachment of reporters for rotation that are small enough to allow undisturbed subunit movement during catalysis. We met these requirements by incorporating F_0F_1 into a liposome and by specifically labeling the b-subunit dimer and the γ subunit with two different fluorophores suitable for single-molecule FRET. To exclude specific photophysical effects of the dyes, we used two alternative FRET donor fluorophores, either tetramethylrhodamine-maleimide (TMR) or rhodamine110-maleimide (Rh110) bound to the γ subunit at residue 106 (**Fig. 1a**,**b**). The FRET acceptor, the bifunctional cyanine-5-bismaleimide (Cy5bis), crosslinked the two cysteines at position 64 in the b-subunit dimer of F_0F_1, avoiding ambiguity in the location of the dye[18].

To avoid any perturbations from surfaces, the labeled holoenzyme was investigated in freely diffusing liposomes that proved to be fully functional. The catalytic rates of these double-labeled enzymes were $v_S = (23 \pm 3)\ s^{-1}$ for ATP synthesis and $v_H = (67 \pm 6)\ s^{-1}$ for ATP

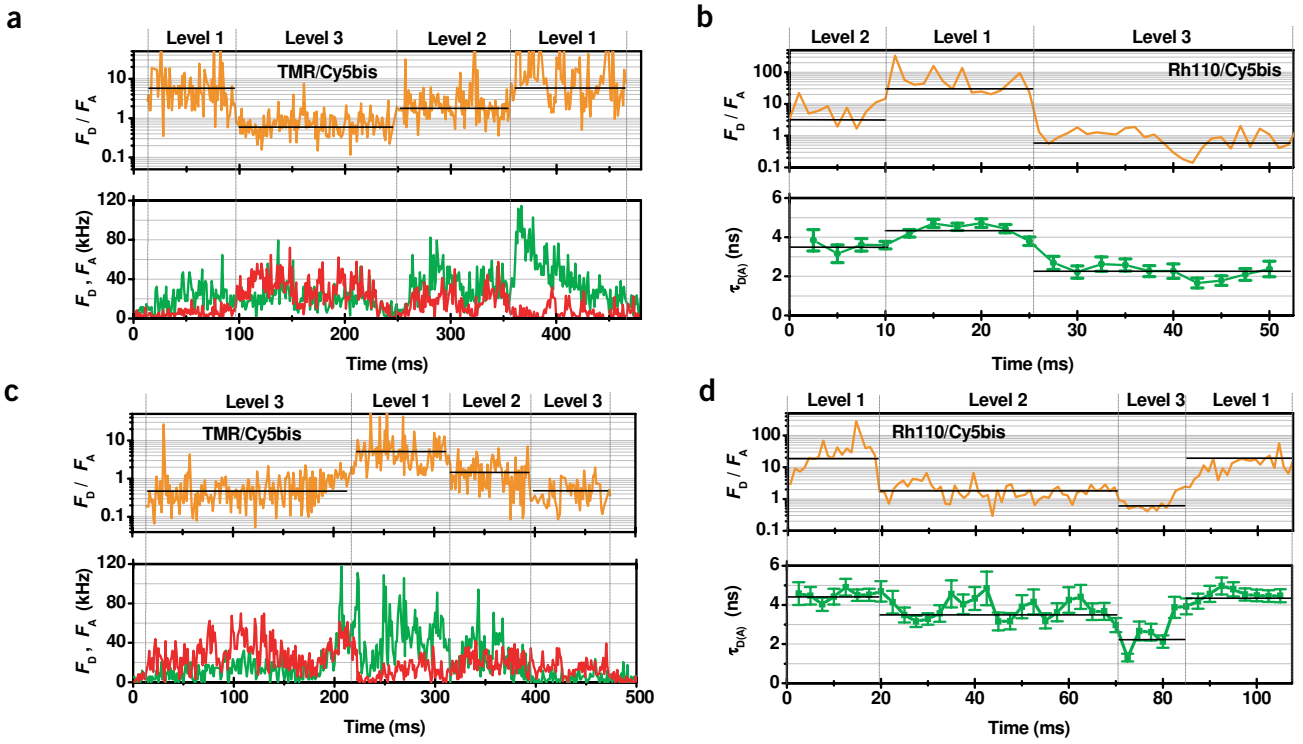

Figure 2 Photon bursts from single F_0F_1-ATP synthases in liposomes. (**a**,**b**) Photon bursts during ATP hydrolysis. (**c**,**d**) Photon bursts during ATP synthesis. FRET donor is TMR in **a** and **c**, Rh110 in **b** and **d**; FRET acceptor is Cy5bis in all traces. Fluorescence intensity traces of the donor, F_D, and acceptor, F_A, are green and red, respectively, in **a** and **c** (time window 1 ms). Corrected intensity ratios F_D / F_A are orange in all panels (time window 1 ms), and fluorescence lifetimes of the donor Rh110 are green in **b** and **d** (total time window 5 ms, shifted by 2.5 ms per data point). Three distinct FRET levels are attributed (1, 2 or 3) at top of panels. Black horizontal lines indicate the mean FRET levels from the distributions in **Figure 4** (additional traces are shown in **Supplementary Fig. 2** online).

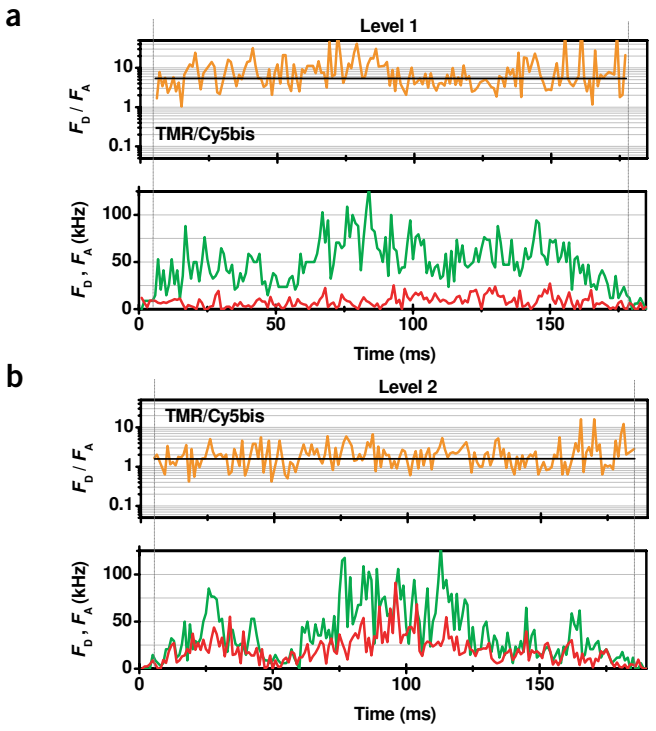

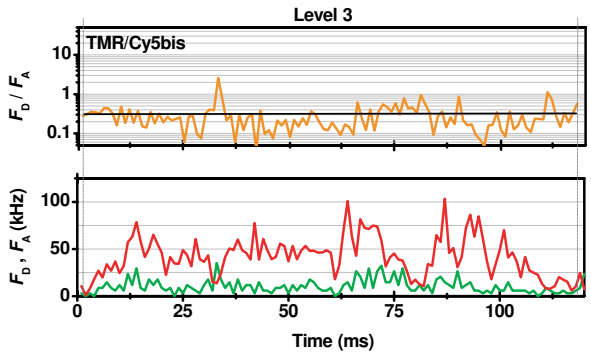

Figure 3 Photon bursts from single liposomes with one double-labeled F_0F_1-ATP synthase in the presence of 1 mM AMPPNP. Fluorescence intensity traces of donor (TMR), F_D, are green, those for the acceptor (Cy5bis), F_A, red. The corrected intensity ratios F_D / F_A are orange (top), showing a constant level within one photon burst. (**a**–**c**) The enzyme is trapped in level 1 (**a**), level 2 (**b**) or level 3 (**c**).

hydrolysis, both of which are similar to those of the unlabeled F_0F_1-ATP synthase[19,20]. Upon addition of 40 μM of the inhibitor *N*,*N*′-dicyclohexylcarbodiimide (DCCD), ATP synthesis was reduced to $v_S = (4 \pm 3)\ s^{-1}$ and ATP hydrolysis to $v_H = (2 \pm 2)\ s^{-1}$, confirming that catalysis was coupled to proton transport[21,22].

Stepwise γ-subunit rotation during ATP hydrolysis

First, we analyzed rotary movements during ATP hydrolysis in the presence of 1 mM ATP. Using intramolecular single-molecule FRET[18,23,24] and single-molecule multiparameter fluorescence detection[25], we obtained quantitative fluorescence information (intensity, lifetime and anisotropy in two spectral regions) from the attached reporters at high time resolution. Single FRET-labeled enzymes incorporated into liposomes were detected by their fluorescence photon bursts while traversing the confocal detection volume (**Fig. 1c**). **Figure 2a** shows a long-lasting photon burst with large fluctuations of the fluorescence intensities of donor, F_D (green) and acceptor, F_A (red). The ratio of corrected fluorescence intensities F_D / F_A was calculated (**Fig. 2**) to correlate these fluctuations with changes in the intramolecular FRET efficiency; that is, with distance changes between the two fluorophores. For the observed photon bursts, we found three different constant levels of F_D / F_A (levels 1, 2 and 3) corresponding to three distinct distances between the labels at the γ and b subunits. These FRET states interchanged in sudden jumps among the levels, with a transition time faster than the time resolution (binning time 1 ms). The burst in **Figure 2a** shows a sequence of four steps of the F_D / F_A levels.

In addition, time traces of the fluorescence lifetime of the donor in the presence of the acceptor, $\tau_{D(A)}$, were simultaneously measured (**Fig. 2b**). Each F_D / F_A level corresponded to a well-defined $\tau_{D(A)}$: high FRET efficiencies (level 3, short distance) were characterized by a short $\tau_{D(A)}$, medium FRET efficiencies (level 2, medium distance) by a larger $\tau_{D(A)}$, and low FRET efficiencies (level 1, long distance) by high ratios of F_D / F_A and a long $\tau_{D(A)}$. The coincident steps in the levels of F_D / F_A and $\tau_{D(A)}$ proved that these jumps were caused by changes in FRET efficiencies and not by temporary photophysical effects[25] of the reporter dyes. FRET levels changed within a single photon burst during ATP hydrolysis in the order 1→3→2→1 (**Fig. 2a**) and 2→1→3 (**Fig. 2b**), respectively. By analyzing 222 traces of single F_0F_1-ATP synthases with two or more FRET levels, the predominant sequence of level transitions was found to be 1→3→2→1→... and so forth for >72% of the bursts. We conclude that during ATP hydrolysis at high ATP concentrations this interconversion of well-defined FRET levels clearly indicates a three-step rotary movement of the γ subunit in membrane-integrated F_0F_1-ATP synthase.

The fact that not all bursts exhibited the same sequence is due to the fast kinetics of ATP hydrolysis. In our analysis, only levels with duration of at least 5 ms were considered separate levels. From the average ATP turnover time and assuming an exponential distribution of the F_D / F_A level durations, we calculated a probability of 77% for levels that last for 5 ms or longer and thus are recognized as distinct levels during ATP hydrolysis. Therefore, apparently 'wrong' sequences were observed because short F_D / F_A levels were sometimes missed.

Stepwise γ-subunit rotation during ATP synthesis

To monitor subunit movements during ATP synthesis, we generated a transmembrane pH difference (ΔpH) plus an additional electric potential difference (Δϕ) across the liposome membrane[19,20] immediately before fluorescence measurements. In **Figure 2c,d**, typical photon bursts of TMR/Cy5bis- and Rh110/Cy5bis-labeled ATP synthases are shown (for additional traces see **Supplementary Fig. 2c,d** online). Three distinct FRET levels were identified within these photon bursts, characterized by constant F_D / F_A and $\tau_{D(A)}$ levels, which interchange in coincident jumps to the next level. After mixing the two buffers in the microscopic flow chamber, ΔpH and Δϕ with initial maximum values dissipated within 3–5 min, partly used by F_0F_1- ATP synthase for ATP synthesis and parly lost in a distinct process by proton leakage across the lipid membrane. Therefore, fluctuating FRET efficiencies within the photon bursts of liposome-embedded ATP synthase were observable only for the first few minutes. Several minutes after mixing, FRET states of F_0F_1 remained constant within the bursts. Rarely, oscillations between two FRET states were detected.

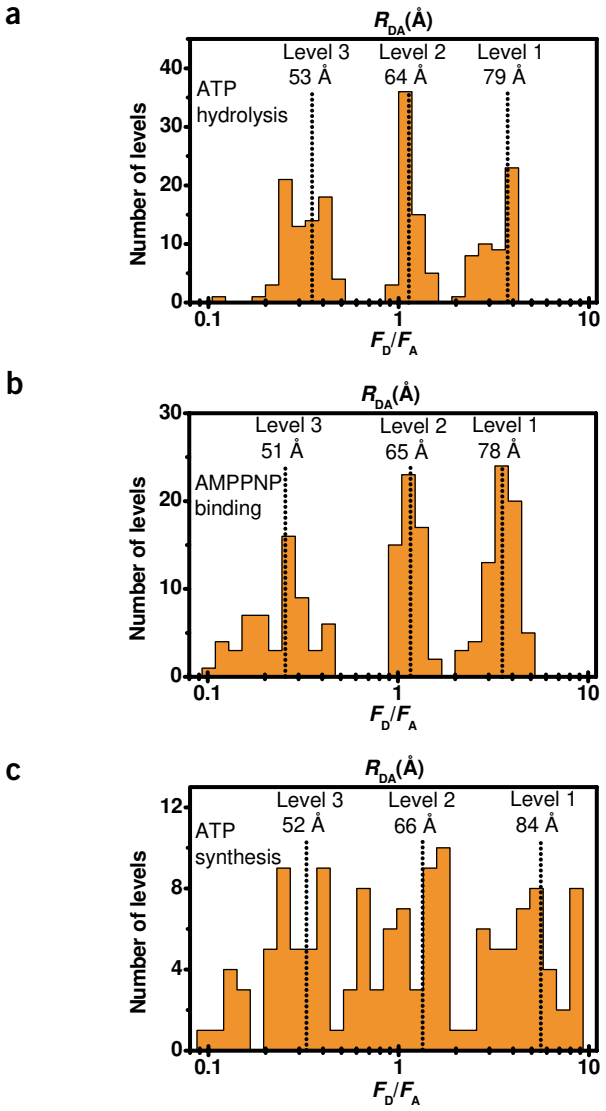

Figure 4 Histograms of the fluorescence intensity ratios F_D / F_A of single FRET-labeled F_0F_1. Top, most probable donor-acceptor distances, R'_{DA} (see Methods). (**a**) During ATP hydrolysis (1 mM ATP), 48 photon bursts with three or more steps (that is, 207 FRET level altogether) were analyzed. (**b**) Binding of AMPPNP (1 mM) with data from 185 photon bursts. (**c**) During ATP synthesis (100 μM ADP, 5 mM phosphate, initial ΔpH = 4.1), 32 photon bursts containing three or more steps (that is, 129 FRET level altogether) were analyzed.

In contrast to ATP hydrolysis, the order of level transitions was reversed for both pairs of FRET fluorophores. The observed sequences are 3→1→2→3 (**Fig. 2c**) and 1→2→3→1 (**Fig. 2d**), respectively. Repeating F_D/F_A and $\tau_{D(A)}$ sequences in the direction 1→2→3→1→... were found for >83% of 188 analyzed bursts with two or more FRET levels. As the sequence of FRET levels is reversed, we conclude that the direction of γ rotation during ATP synthesis is opposite compared with that during ATP hydrolysis.

Three AMPPNP-trapped γ-subunit orientations

The existence of three distinct FRET levels was corroborated by an independent experiment. Upon addition of nonhydrolyzable adenosine-5′-(β,γ-imido)triphosphate (AMPPNP) the enzyme was expected to be trapped in one of three different orientations of the γ subunit with respect to the b subunits. In this case, the traces of single-particle events showed F_D / F_A levels that remained constant throughout each burst. The observation of three distinct FRET efficiencies upon addition of AMPPNP supports the proper discrimination of the anticipated γ-subunit orientations (**Fig. 3a–c**).

Level histograms of the three FRET states

The statistical significance of the individual traces of F_0F_1 was evaluated by the analysis of the FRET level histograms of ATP synthases during catalysis and AMPPNP binding (**Fig. 4**). We selected 48 photon bursts from single F_0F_1 with three or more FRET levels during ATP hydrolysis. In the histogram of F_D / F_A levels (**Fig. 4a**), three peaks are clearly separated. In **Figure 4b**, the F_D / F_A level histogram in the presence of AMPPNP is shown. Three F_D / F_A levels are found also, with the center of the distribution of each level similar to those observed during ATP hydrolysis. At millimolar concentrations, ATP binds rapidly to the free nucleotide-binding site and the rate-limiting step is expected to be the release of ADP. The resting positions of the enzyme should therefore be the same as those after binding of AMPPNP, resulting in almost identical maxima of the F_D / F_A level histograms in the presence of ATP or AMPPNP.

The histogram of F_D / F_A levels, obtained from of 32 photon bursts during ATP synthesis (**Fig. 4c**), shows again three subpopulations. When F_D / F_A level distributions are fitted with three Gaussians, the centers of the distributions are almost identical to those for ATP hydrolysis and AMPPNP binding. In the case of ATP synthesis, the maxima of the distribution were similar; however, the distributions were significantly broadened.

Dwell times of the FRET states during catalysis

The durations of the different F_D / F_A levels during ATP hydrolysis and ATP synthesis were considered as dwell times of conformational states. A monoexponential fit to the level durations during ATP hydrolysis resulted in an average dwell time of 19 ms (**Fig. 5a**). This value agrees well with a turnover time of 15 ms for the hydrolysis of one ATP obtained from bulk experiments. For ATP synthesis, a monoexponential fit to the level durations yielded an average dwell time of 51 ms (**Fig. 5b**), in accordance with a turnover time of 43 ms for the synthesis of one ATP calculated from the initial rates in bulk experiments. This comparison indicates that the duration of the FRET states is directly correlated with the catalytic event.

Fluorophore distances and γ-subunit orientations

Single-molecule FRET data revealed additional structural information. From the homology model of F_0F_1 (**Fig. 1**), the largest distance between the Cα atoms of the amino acids b-Q64C and γ-T106C was estimated to be 73 Å. Rotation of the γ subunit by 120° and 240° resulted in two shorter distances in the range of 40–60 Å. According to the Förster theory of FRET[26,27], two effects can influence F_D / F_A levels, donor-acceptor distances and orientations in transition dipole moments (factor κ^2) of the donor relative to the acceptor dye. We calculated apparent donor-acceptor distances, R'_{DA}, from the measured fluorescence parameters. These apparent distances of 52, 65 and 80 Å (**Fig. 4**), representing mean values during catalysis and AMPPNP binding for the three FRET states within the enzyme, agree with estimates obtained from the model.

DISCUSSION

We applied an intramolecular single-molecule FRET approach to show subunit rotation in the liposome-reconstituted holoenzyme F_0F_1-ATP

synthase powered by proton flow. Here, one fluorophore was attached to the rotating γ subunit of F_1 and the other to the static, nonrotating b-subunit dimer of F_0. We achieved high-specificity labeling by separately labeling cysteines in F_1 and F_0 and subsequently reassembling and reconstituting the enzyme into liposomes. The FRET efficiency depends on the distance between the two fluorophores. Therefore, FRET efficiency changes between the two fluorophores at a single ATP synthase are expected to describe trajectories of the relative motion of the two labeled subunits during catalysis.

Upon addition of AMPPNP as a nonhydrolyzable substrate for the enzyme, we find three well-defined and distinct FRET levels and conclude that these levels correspond to three distances of the labeled residue 106 at a protruding part ('off-axis position') of the γ subunit with respect to the b subunits. The calculated ratio of corrected fluorescence intensities F_D / F_A between FRET donor and acceptor in the photon bursts of a single ATP synthase is independent of intensity fluctuations of the double-labeled enzyme on its transit pathway through the confocal detection volume. In addition to this intensity ratio, each FRET level is defined by a specific FRET donor fluorescence lifetime $\tau_{(DA)}$, and therefore, other photophysical causes effecting the quantum yields of the FRET fluorophores are unlikely. These stable FRET levels during a photon burst indicate the trapping of the γ subunit by AMPPNP in one of three distinguishable orientations. The three intramolecular distances calculated from the FRET efficiencies of these levels are in good agreement with the distances derived from our model of F_0F_1-ATP synthase and the expected positions of the γ subunit.

FRET-labeled ATP synthase in a freely diffusing liposome carries out proton transport-coupled ATP synthesis and hydrolysis almost undisturbed during real-time observation. The dwell times of the FRET levels correspond to the bulk rates of catalysis, during ATP hydrolysis as well as ATP synthesis, thereby independently excluding photophysical causes for interchanging FRET levels.

Given this direct correlation between FRET level and γ-subunit orientation, γ-subunit rotation in F_0F_1-ATP synthase occurs stepwise in both modes of catalysis and the direction of rotation during ATP synthesis is reversed compared with that during ATP hydrolysis. Using the actin-filament method, the rotation direction of the γ subunit in F_1 subcomplexes during ATP hydrolysis has been determined to be counterclockwise when viewed from F_0 (ref. 9). Therefore we attribute the FRET level sequence 1→3→2→1→... observed during ATP hydrolysis to the counterclockwise direction of rotation of the γ subunit (**Fig. 1b**). Stepwise rotation of the γ subunit during ATP hydrolysis has been discussed for F_1-ATPase[10,11,28] and for F_0F_1-ATP synthase[18] earlier and is confirmed here. In the present work, proton-driven ATP synthesis is also accompanied by a three-step rotary movement of the γ subunit and not by a quasi-continuous rotation, which might have been expected from the stoichiometry of at least nine translocated protons per 360° revolution and from the multistep rotational motion of the c subunits of F_0 during ATP synthesis. These distinct distances between the FRET fluorophores remain constant throughout the dwell time of one γ-subunit orientation, before a consecutive 120° rotary movement of the γ subunit takes place, as has been shown unequivocally with immobilized F_1 subcomplexes for the case of ATP hydrolysis at millimolar concentrations[10]. The mean stopping positions of the γ subunit upon ATP synthesis are similar to those observed in the AMPPNP-trapped states and those during ATP hydrolysis at millimolar ATP concentrations.

As anticipated in molecular dynamics simulations[15,16] and derived from theoretical considerations of microscopic reversibility, a reversed rotary motion of the γ subunit during ATP synthesis was predicted,

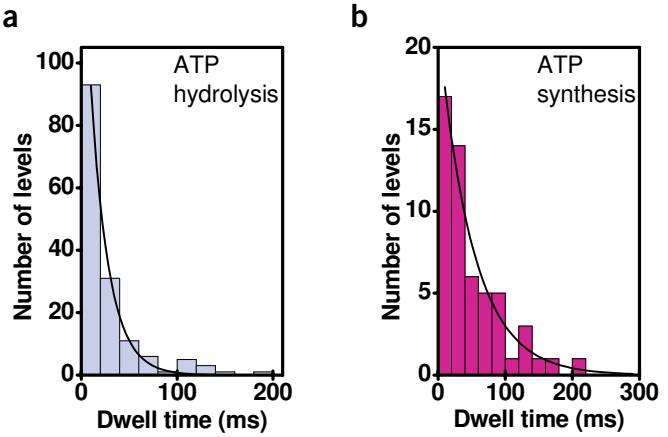

Figure 5 Level duration distributions of FRET states. (**a**,**b**) Distributions during ATP hydrolysis (**a**) and ATP synthesis (**b**). Fits with monoexponential decay functions yield mean dwell times of 19 ms upon ATP hydrolysis and 51 ms upon ATP synthesis.

and is now strongly supported by our experiments. The rotary subunit movement is indicated by repeating sequences of three FRET levels, which are induced by distance changes between the FRET pair. In most cases, a consecutive order of the three γ-subunit orientations was observed, and in an opposite direction during ATP synthesis from that during ATP hydrolysis. Thus, unidirectional rotary motion of the γ subunit during both modes of catalysis seems very improbable. Any two-state model, including contracting-and-stretching modes of the γ subunit or back-and-forth swiveling modes between only two of the three catalytic sites, are not consistent with the repeating sequences of three FRET levels. Oscillations between two FRET states were rarely observed and can be attributed either to omitted levels or to an equilibrium state between a weak proton-motive force competing with the ATP hydrolysis backreaction.

The significant broadening of the three FRET levels during ATP synthesis allows us to predict the occurrence of substeps comparable to those observed in F_1 subcomplexes during ATP hydrolysis. As first hints and as rare events we identified more than three FRET levels (substeps) in some photon bursts of F_0F_1 during ATP synthesis. The origin of these substeps remains to be clarified. In principle, a hypothetical ADP-(plus P_i)-waiting state of the enzyme at one angular position of the γ subunit and a conformational state associated with the catalytic reaction or product release at another angular position can be discriminated by the dependence of substrate concentration. Detecting one ATP synthase in freely diffusing liposomes, as has been shown in this work, limits the observation time to several hundred milliseconds. Therefore, concentration dependencies must be studied by a modified approach, for instance with surface-immobilized liposomes using a streptavidin-biotin multilayer. Monitoring single enzymes at work under kinetic control in both directions of catalysis will reveal insights into the mechanism of the 'rotary nanomachine' F_0F_1-ATP synthase.

METHODS

FRET-labeled F_0F_1-ATP synthase from *E. coli*. F_1 of ATP synthase of *E. coli* carrying the cysteine mutation γ-T106C was prepared as described[29] using the plasmid pRA144 (ref. 30) expressed in strain RA1 (ref. 31). Specific substoichiometric labeling of the γ subunit was achieved with tetramethylrhodamine-maleimide (TMR, Molecular Probes) or Rhodamine110-maleimide (Rh110, Evotec) with labeling efficiencies between 50 and 60% (refs. 18,32). F_1 with

γ-T106C contains several buried cysteines[33]. However, at the given reaction conditions only γ-T106C is labeled[32,33], as checked by fluorograms after SDS-PAGE. F_0F_1-ATP synthases of *E. coli* carrying the cysteine mutation b-Q64C were prepared separately[19] using the plasmid pRR76 (ref. 18) expressed in strain RA1. The cysteines of the b subunits were crosslinked with the cyanine dye Cy5-bis-C_5-maleimide synthesized from (5-maleimidyl)-pentyl-1-amine and Cy5-bis-*N*-hydroxysuccinimidylester (bisreactive Cy5 NHS-ester obtained from Amersham Biosciences). Cy5-labeling efficiency of the b-subunit dimer was 64% with a yield of crosslinking of ~90%. The a and c subunits of F_0 were not labeled as checked by fluorograms after SDS-PAGE. Cy5-labeled F_0F_1 was reconstituted into liposomes (diameter ~100 nm), F_1 was removed and Cy5-labeled F_0 was reassembled with TMR- or Rh110-labeled F_1 to yield the FRET-labeled F_0F_1-ATP synthase in liposomes, as described[18]. ATP synthesis rates were measured[19,20] at 23 °C, yielding $v_S = 59 \pm 1\ s^{-1}$ for the nonlabeled b-mutant F_0-b64-F_1, $v_S = 48 \pm 3\ s^{-1}$ for the labeled F_0-b64-Cy5–F_1, $v_S = 24 \pm 2\ s^{-1}$ for the reassembled TMR-labeled F_0-b64–F_1-γ106-TMR and $v_S = 23 \pm 3\ s^{-1}$ for the FRET-labeled F_0-b64-Cy5–F_1-γ106-TMR. ATP hydrolysis rates at 23 °C were $v_H = 186 \pm 12\ s^{-1}$ for F_0-b64–F_1, $v_H = 108 \pm 24\ s^{-1}$ for F_0-b64-Cy5–F_1 and $v_S = 67 \pm 6\ s^{-1}$ for the reassembled and FRET-labeled F_0-b64-Cy5–F_1-γ106-TMR. Reassembly causes slower rates[18,21]. All hydrolysis rates were inhibited by 40 μM DCCD to remaining activities of 6 ± 4%.

Single-molecule FRET measurements. Single-molecule FRET measurements were carried out as described[18] using continuous wave-excitation at 532 nm for TMR and pulsed excitation at 496 nm for Rh110. Confocal detection volumes of 6.8 fl for TMR/Cy5bis and 2.5 fl for Rh110/Cy5bis were used. Mean diffusion times through the confocal volume of 10–30 ms for the labeled F_0F_1 in liposomes were determined by fluorescence correlation spectroscopy. Single-molecule fluorescence measurements under conditions of ATP hydrolysis (1 mM ATP) and AMPNP binding (1 mM AMPPNP) were carried out in a buffer (pH 8) containing 20 mM succinic acid, 20 mM tricine, 2.5 mM $MgCl_2$, 80 mM NaCl and 0.6 mM KCl. ATP synthesis was measured after preincubation of the liposomes in 20 mM succinic acid buffer, pH 4.7, containing 5 mM NaH_2PO_4, 0.6 mM KOH, 2.5 mM $MgCl_2$, 100 μM ADP, 20 μM valinomycin. The transmembrane ΔpH was generated by mixing the acidic liposomes with the basic buffer containing 200 mM tricine, pH 8.8, 5 mM NaH_2PO_4, 160 mM KOH, 2.5 mM $MgCl_2$ and 100 μM ADP in a T-shaped flow chamber with two syringes. This generated an initial transmembrane pH difference ΔpH = 4.1 with an additional electric potential difference Δϕ = 126 mV (refs. 19,20). All samples of the double-labeled F_0F_1 were diluted to a final concentration of ~90 pM.

F_0F_1 identification in photon bursts. Background count rates (usually between 0.5 and 2 kHz), obtained in each experiment from measurements of buffer solutions without labeled enzymes, were subtracted from the burst count rates. In addition, crosstalk (photons from the donor in the detection channel of the acceptor) and differences in the detection efficiencies of the donor and acceptor channels of the instrument were corrected, resulting in corrected fluorescence intensities for donor (F_D) and acceptor (F_A). A photon burst was considered 'significant' when the sum of photon counts in the donor and acceptor channel was >15 counts per ms. To eliminate events of remaining donor-labeled F_1 that were not bound to F_0 in liposomes, we excluded photon bursts with a duration <45 ms and, when Rh110 was used, with a donor anisotropy <0.12 (see **Supplementary Fig. 1** online).

Calculation of intramolecular FRET distances. The reduced Förster radii[25] $R_{0r} = 9{,}780\ (J(\lambda)\ \kappa^2\ n^{-4})^{1/6}$ for the FRET pairs TMR/Cy5bis and Rh110/Cy5bis were calculated using $n = 1.33$ for the index of refraction and $\kappa^2 = 2/3$. The spectral overlap (J) was determined from the respective donor emission and acceptor absorption spectra resulting in $R_{0r} = 76$ Å for TMR/Cy5bis and 55.5 Å for Rh110/Cy5bis. Anisotropies of donor and acceptor were 0.2. Even in this case, it is still sufficient to assume $\kappa^2 = 2/3$, because our estimate for κ^2 lies well in the range of possible κ^2 values assuming the case of linear and planar (due to rotation) transition moments of donor and acceptor[27]. Based on these assumptions, it is appropriate to calculate apparent donor-acceptor distances, R'_{DA} from the measured fluorescence parameters using $R'_{DA} = R_{0r}\ [\phi_A\ (F_D / F_A)]^{1/6}$.

The apparent distances between donor and acceptor dyes were calculated from the maxima of the Gaussian distributions of F_D / F_A for the different levels. The effective acceptor fluorescence quantum yield in single-molecule experiments was $\phi_A = 0.32$ for Cy5bis[25]. These distances are compared with geometrically estimated values from a model of F_0F_1. Therefore, homology alignment[34] of structures of the ($\alpha_3\beta_3\gamma$) subcomplex from the mitochondrial enzyme, δ, ε plus γ and c subunits from X-ray[3,35] and NMR[36,37] analyses were combined with postulated structures of the c_{10}-ring[8] and a and b subunits[38] for an overview of intramolecular distances within F_0F_1-ATP synthase.

Note: Supplementary information is available on the Nature Structural & Molecular Biology website.

ACKNOWLEDGMENTS

This work is dedicated to the memory of K. Süss, who died on 17 March 2002. We thank R.H. Fillingame for his help with the b-mutants, R.A. Capaldi and R. Aggeler for the gift of the γ-mutant, O. Hucke for refinement of the F_0F_1 model, and M. Antonik and E. Haustein for analytical software. We thank H. Grubmüller, R. Jahn, B.A. Melandri and P. Turina for critical reading the manuscript and helpful discussions and A. Börsch-Haubold for editorial suggestions. C.A.M.S. acknowledges financial support by the Bundesministerium für Bildung und Forschung (BioFuture grant 0311865).

COMPETING INTERESTS STATEMENT

The authors declare that they have no competing financial interests.

Received 12 September; accepted 12 November 2003
Published online at http://www.nature.com/natstructmolbiol/

1. Mitchell, P. Coupling of phosphorylation to electron and hydrogen transfer by chemiosmotic type of mechanism. *Nature* **191**, 144–152 (1961).
2. Boyer, P.D. ATP synthase—past and future. *Biochim. Biophys. Acta* **1365**, 3–9 (1998).
3. Abrahams, J.P., Leslie, A.G.W., Lutter, R. & Walker, J.E. Structure at 2.8 Å resolution of F_1-ATPase from bovine heart mitochondria. *Nature* **370**, 621–628 (1994).
4. Junge, W., Sabbert, D. & Engelbrecht, S. Rotatory catalysis by F-ATPase: Real-time recording of intersubunit rotation. *Ber. Bunsenges. Phys. Chem.* **100**, 2014–2019 (1996).
5. Yoshida, M., Muneyuki, E. & Hisabori, T. ATP synthase – a marvelous rotary engine of the cell. *Nat. Rev. Mol. Cell. Biol.* **2**, 669–677 (2001).
6. Capaldi, R.A. & Aggeler, R. Mechanism of the F_1F_0-type ATP synthase, a biological rotary motor. *Trends Biochem. Sci.* **27**, 154–160 (2002).
7. Weber, J. & Senior, A.E. ATP synthesis driven by proton transport in F_1F_0-ATP synthase. *FEBS Lett.* **545**, 61–70 (2003).
8. Fillingame, R.H., Angevine, C.M. & Dmitriev, O.Y. Coupling proton movements to c-ring rotation in F_1F_0 ATP synthase: aqueous access channels and helix rotations at the a-c interface. *Biochim. Biophys. Acta* **1555**, 29–36 (2002).
9. Noji, H., Yasuda, R., Yoshida, M. & Kinosita, K. Jr. Direct observation of the rotation of F_1-ATPase. *Nature* **386**, 299–302 (1997).
10. Yasuda, R., Noji, H., Yoshida, M., Kinosita, K. & Itoh, H. Resolution of distinct rotational sub-steps by submillisecond kinetic analysis of F_1-ATPase. *Nature* **410**, 898–904 (2001).
11. Yasuda, R. *et al.* The ATP-waiting conformation of rotating F_1-ATPase revealed by single-pair fluorescence resonance energy transfer. *Proc. Natl. Acad. Sci. USA* **100**, 9314–9318 (2003).
12. Sambongi, Y. *et al.* Mechanical rotation of the c subunit oligomer in ATP synthase (F_0F_1): direct observation. *Science* **286**, 1722–1724 (1999).
13. Junge, W. *et al.* Inter-subunit rotation and elastic power transmission in F_0F_1-ATPase. *FEBS Lett.* **504**, 152–160 (2001).
14. Kaim, G. *et al.* Coupled rotation within single F_0F_1 enzyme complexes during ATP synthesis or hydrolysis. *FEBS Lett.* **525**, 156–163 (2002).
15. Böckmann, R.A. & Grubmüller, H. Nanosecond molecular dynamics simulation of primary mechanical energy transfer steps in F_1-ATP synthase. *Nat. Struct. Biol.* **9**, 198–202 (2002).
16. Ma, J. *et al.* A dynamical analysis of the rotation mechanism for conformational change in F_1-ATPase, *Structure* **10**, 921–930 (2002).
17. Zhou, Y., Duncan, T.M., Cross, R.L. Subunit rotation in *Escherichia coli* F_0F_1-ATP synthase during oxidative phosphorylation. *Proc. Natl. Acad. Sci.* USA **94**, 10583-10587 (1997).
18. Börsch, M., Diez, M., Zimmermann, B., Reuter, R. & Gräber, P. Stepwise rotation of the γ-subunit of EF_0F_1-ATP synthase observed by intramolecular single-molecule fluorescence resonance energy transfer, *FEBS Lett.* **527**, 147–152 (2002).
19. Fischer, S. & Gräber, P. Comparison of ΔpH- and Δϕ-driven ATP synthesis catalyzed by the H^+-ATPases from *Escherichia coli* or chloroplasts reconstituted into liposomes. *FEBS Lett.* **457**, 327–332 (1999).
20. Fischer, S., Gräber, P. & Turina, P. The activity of the ATP synthase from *Escherichia coli* is regulated by the transmembrane proton motive force. *J. Biol. Chem.* **275**, 30157–30162 (2000).
21. Lötscher, H.R., deJong, C. & Capaldi, R.A. Modification of the F_0 portion of the H^+-

translocating adenosinetriphosphatase complex of *Escherichia coli* by the water-soluble carbodiimide 1-ethyl-3-[3-(dimethylamino)propyl]carbodiimide and effect on the proton channeling function. *Biochemistry* **23**, 4128–4134 (1983).
22. Perlin, D.S., Cox, D.N. & Senior, A.E. Integration of F_1 and the membrane sector of the proton-ATPase of *E. coli*. *J. Biol. Chem.* **258**, 9793–9800 (1983).
23. Weiss, S. Measuring conformational dynamics of biomolecules by single molecule fluorescence spectroscopy. *Nature Struct. Biol.* **7**, 724–729 (2000).
24. Ha, T. Single-molecule fluorescence resonance energy transfer. *Methods* **25**, 78–86 (2001).
25. Rothwell, P.J. *et al.* Multi-parameter single-molecule fluorescence spectroscopy reveals heterogeneity of HIV-1 reverse transcriptase: primer/template complexes. *Proc. Natl. Acad. Sci. USA* **100**, 1655–1660 (2003).
26. Förster, T. Zwischenmolekulare Energiewanderung und Fluoreszenz. *Ann. Phys.* **2**, 55–70 (1948).
27. Van der Meer, B.W., Cooker, G. & Chen, S.S.-Y. *Resonance Energy Transfer: Theory and Data* (VCH, New York, 1994).
28. Häsler, K., Engelbrecht, S. & Junge, W. Three-stepped rotation of subunits Q and O in single molecules of F-ATPase as revealed by polarized, confocal fluorometry. *FEBS Lett.* **426**, 301–304 (1998).
29. Gogol, E.P., Luecken, U., Bork, T. & Capaldi, R.A. Molecular architecture of *Escherichia coli* F1 adenosinetriphosphatase. *Biochemistry* **28**, 4709–4716 (1989).
30. Aggeler, R. & Capaldi, R.A. Cross-linking of the γ subunit of the *Escherichia coli* ATPase (ECF_1) via cysteines introduced by site-directed mutagenesis. *J. Biol. Chem.* **267**, 21355–21359 (1992).
31. Aggeler, R., Ogilvie, I. & Capaldi, R.A. Rotation of a γ-ε subunit domain in the *Escherichia coli* F_1F_0-ATP synthase complex. *J. Biol. Chem.* **272**, 19621–19624 (1997).
32. Börsch, M. *et al.* Conformational changes of the H^+-ATPase from *Escherichia coli* upon nucleotide binding detected by single molecule fluorescence. *FEBS Lett.* **437**, 251–254 (1998).
33. Turina, P. & Capaldi, R.A. ATP hydrolysis-driven structural changes in the γ-subunit of *Escherichia coli* ATPase monitored by fluorescence from probes bound at introduced cysteine residues. *J. Biol. Chem.* **269**, 13465–13471 (1994).
34. Engelbrecht, S. & Junge, W. ATP synthase: a tentative structural model**.** *FEBS Lett.* **414**, 485–491 (1997).
35. Rodgers, A. & Wilce, M. Structure of the γ/ε complex of ATP synthase: the camshaft in the rotary motor of life. *Nat. Struct. Biol.* **7**, 1051–1054 (2000).
36. Wilkens, S., Dunn, S., Chandler, J., Dahlquist, F.W. & Capaldi, R.A. Solution structure of the N-terminal domain of the δ subunit of the *E. coli* ATP synthase (ECF_1F_0). *Nat. Struct. Biol.* **4**, 198–201 (1997).
37. Girvin, M.E., Rastogi, V.K., Abildgaard, F., Markley, J.L. & Fillingame, R.H. Solution structure of the transmembrane H^+-transporting subunit c of the F_0F_1 ATP synthase. *Biochemistry.* **37**, 8817–8824 (1998).
38. Del Rizzo, P.A., Dunn, S.D., Bi, Y. & Shilton, B.H. The 'second stalk' of *Escherichia coli* ATP synthase: structure of the isolated dimerization domain. *Biochemistry* **41**, 6875–6884 (2002).